A CRITERION BASED ON THE CALCULATION OF A SOLID ANGLE TO ASSESS THE QUALITY OF ACOUSTIC IMAGES OBTAINED WITH A SMA

Kevin Rouard*[1], Julien St-Jacques[1], Franck Sgard[2], Olivier Doutres[1], Hugues Nélisse[2], Loic Boileau[3], Alain Berry[3], Nicolas Quaegebeur[3], François Grondin[3] and Thomas Padois†[2]

[1]École de technologie supérieure (ÉTS), 1100 Rue Notre Dame O., Montréal, QC, H3C 1K3, Canada
[2]Institut de recherche Robert-Sauvé en santé et en sécurité du travail (IRSST), 505 Boulevard de Maisonneuve O., Montréal, QC, H3A 3C2, Canada
[3]Université de Sherbrooke (UdeS), 2500, Boulevard de l'Université, Sherbrooke, QC, J1K 2R1, Canada

1 Introduction

Beamforming algorithm makes it possible to estimate both the direction and the level of the sound sources. Sources are depicted by color spots in an acoustic image. Color spots represent lobes, with the mainlobe identifying the source position, while sidelobes correspond to spurious sources resulting from the array design. Various criteria exist to assess the quality of an acoustic image and, by extension, the efficiency of an array design and the associated algorithm. The level of the source (is indicated by the mainlobe) [1], the level of the mainlobe-to-sidelobe ratio (MSR) [2], and the area ratio of the mainlobe and occasional sidelobes in the acoustic image, known as the spatial resolution [3], are well-established criteria. Several methods are used to calculate the area ratio of the presence of the lobes with respect to the total area of the acoustic image. Mainlobes can be uniform or spread, and sidelobes are scattered, which increases the complexity task. For spherical microphone arrays (SMA), the ellipse area can be used, considering a polar projection of a hemisphere [4] or as an ellipse array ratio [5–7]. The area ratio depends on the array design, the algorithm, and the frequency. This paper proposes to compare the solid angle as a spatial resolution criterion in the field of acoustic imaging.

This paper is organized as follows. Details of the numerical simulation are given first. Then, the covariance ellipse and the solid angle are described. Third, both ellipse area and solid angle as criterion are compared. Finally, Discussion and conclusion are provided in the last section.

2 Methodology

2.1 Numerical simulation

A numerical simulation is conducted in a free-field environment with a rigid SMA and a t-design geometry of 36 microphones [8]. The SMA is located 2 meters away from a monopole that emits a pure tone. In the following, the frequency is represented as kr, a dimensionless number, where k is the wavenumber and r is the radius of the sphere. Several positions of monopoles are considered: directly in front of the SMA ($\theta = 90°, \phi = 0°$), in front of the SMA near the floor ($\theta = 45°, \phi = 0°$) and almost behind the SMA near the floor ($\theta = 45°, \phi = 135°$). Spherical harmonics are used to obtain the sound pressure at each microphone, then the SHB algorithm is used to obtain the acoustic image [6]. The scan zone is a grid of points 90×180, respectively in elevation and azimuth, and is applied at 2 m. The ellipse and the solid angle are calculated at -9 dB to further distinguish the two methods and reach the sidelobes. For acoustic images at $kr = 1$ (low frequency) and $kr = 6$ (high frequency), the truncation order N is equal to 2 and 5, respectively.

2.2 Covariance ellipse

Spatial resolution with the covariance ellipse method to assess the area ratio in the acoustic image consists in computing the area of an ellipse whose radii correspond to the eigenvalues of a covariance matrix from the acoustic image data at a chosen dynamic [3]. The computed surface area is then normalized by the theoretical maximum, that is $\pi \times 90^{\circ} \times 180^{\circ}$ in an arbitrary unit and leads to $\overline{S}$.

2.3 Solid angle

The solid angle is a quantitative method used in various scientific fields to assess the spatial dispersion of light, energy, particles, and the apparent size of celestial objects for instance. For acoustic imaging, the spatial resolution with the proposed solid angle is based on the calculation of the ratio of a portion of the sphere's surface area to the square of the sphere's radius. The infinitesimal solid angle is defined as,

$$\mathrm{d}\Omega = \frac{\mathrm{d}S}{r^2} = |\mathrm{d}(\cos\theta)\mathrm{d}\phi|, \tag{1}$$

where θ is the elevation angle, ϕ the azimuth angle and the total solid angle over a sphere is $\int \mathrm{d}\Omega = 4\pi$ in steradian (sr) [9]. Then, Eq. (2) is decomposed into a sum of finite differences and a normalized solid angle is computed from the acoustic image data at a chosen dynamic given by,

$$\overline{\Omega} = \frac{1}{4\pi}\sum_{i}^{I}(-\cos\theta_{i+1} + \cos\theta_i)(\phi_{i+1} - \phi_i), \tag{2}$$

where (θ_i, ϕ_i) are a set of positions around (θ_l, ϕ_l) positions where $l = 1, ..., L$ is the index of a scan grid and $i = 1, ..., I$ is the index of mid-positions around (θ_l, ϕ_l) of a scan grid. The number of scan grid positions is $L = N_\theta \times N_\phi$ and the number of mid-positions is $I = (N_\theta + 2) \times (N_\phi + 2)$ where N is the number of positions per angle. Attention is given to the continuity of the angular periodicity, *i.e.* $\theta = \pi = 0\,[\pi]$ and $\phi = 2\pi = 0\,[2\pi]$, enabling computation on the whole sphere. Thus, the computation around each position (θ_l, ϕ_l) in the acoustic image represents a fraction of the total solid angle.

3 Results

For $kr = 1$ and for the source directly in front of the SMA, (see in Fig. 1.a), the mainlobe is uniform and both meth-

*kevin.rouard.1@ens.etsmtl.ca
†thomas.padois@irsst.qc.ca

ods provide similar values of area ratio: $\overline{S} = 20\,\%$ and $\overline{\Omega} = 19.1\,\%$. In Fig. 1.b) the source is in front of the SMA near the floor and the mainlobe is spread out towards the south pole due to the spherical plane, although it is the same source as before. The normalized ellipse area increases to $48\,\%$, while the normalized solid angle remains stable at $19.2\,\%$. In Fig. 1.c) the source is almost behind the SMA near the floor, the map is similar, but part of the source shape is transferred to the other side of the acoustic image: $\overline{S} = 82.4\,\%$ is larger and $\overline{\Omega} = 19.2\,\%$ remains unchanged. For $kr = 6$, the source is directly in front of the SMA, (see Fig. 1.d), the mainlobe is smaller and two symmetrical sidelobes appear. In this case $\overline{S} = 28.1\,\%$, which is much larger than the solid angle value $\overline{\Omega} = 7.1\,\%$.

The results for $kr = 1$ show that the solid angle method has a low computational error with respect to the position of the source compared to the ellipse method. The ellipse may exceed the acoustic image frame when the mainlobe is distorted around the poles. The ellipse calculates the lobe area from the radii in a plane, while the solid angle considers the spherical plane, and the solid angle reflects the quality of the acoustic image with a SMA. For $kr = 6$ there are sidelobes and the ellipse surrounding them and exceeding the acoustic image frame, which leads to a high value of the criterion, while the solid angle calculates the sum of the emerging lobes at -9 dB, which leads to a lower value. Sidelobes position affects the value of the ellipse, potentially leading to the misinterpretation of a large mainlobe.

In the literature, the acoustic source is often located in front of the SMA and therefore the source is located at the center of the image. In this case and without sidelobes, similar values are found for both methods. In practice, the source may be close to the ground or ceil (toward a pole) or off-axis of a SMA, and in these cases the solid angle is more suitable than the ellipse.

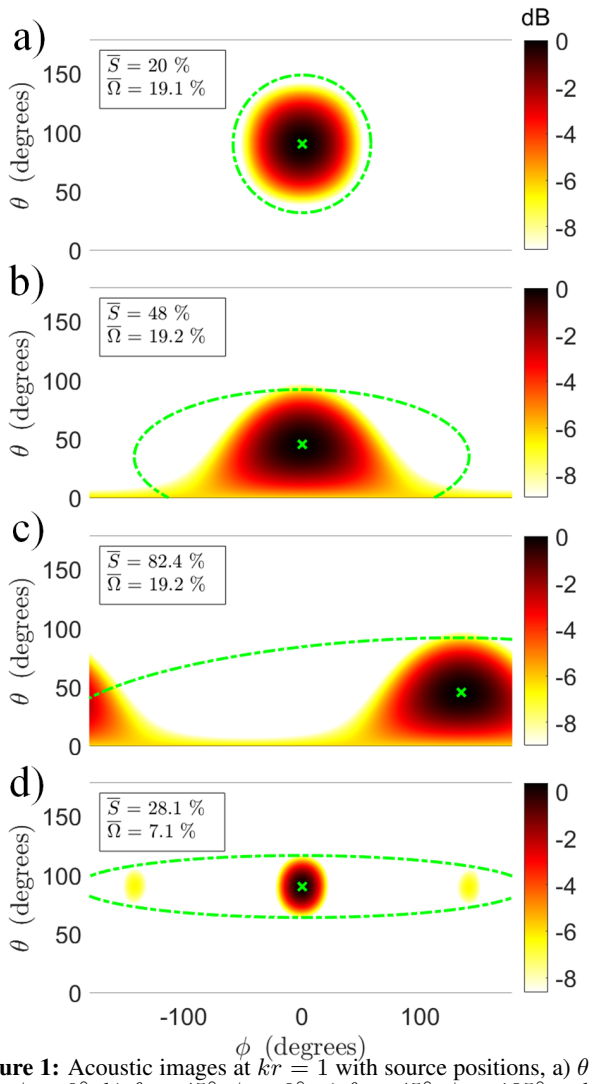

Figure 1: Acoustic images at $kr = 1$ with source positions, a) $\theta = 90°, \phi = 0°$, b) $\theta = 45°, \phi = 0°$, c) $\theta = 45°, \phi = 135°$ and d) at $kr = 6$ with source position $\theta = 90°, \phi = 0°$, the green cross depicted the source position, computed ellipse is depicted in green dashed line and solid angle is computed on displayed colormap.

4 Conclusions

Spatial resolution criteria have been compared, such as the covariance ellipse and the proposed solid angle. Both methods give a similar value when the source is centered in the acoustic image and in low frequency. Differences between these methods occur when the source position is near the edges or when there are sidelobes at high frequency. The values given by the solid angle method, calculated in the spherical plane, are not sensitive to the source position. Therefore, this method is more robust to assess the image quality in the presence of different sources.

References

[1] E. Sarradj. Three-Dimensional Acoustic Source Mapping with Different Beamforming Steering Vector Formulations. *Advances in Acoustics and Vibration*, 2012:1–12, 2012.

[2] P. Chiariotti, M. Martarelli, and P. Castellini. Acoustic Beamforming for Noise Source Localization – Reviews, Methodology and Applications. *MSSP*, 120:422–448, 2019.

[3] T. Padois, J. Fischer, C. Doolan, and O. Doutres. Acoustic Imaging with Conventional Frequency Domain Beamforming and Generalized Cross-correlation: a comparison study. *Applied Acoustics*, 177:107914, 2021.

[4] L. H. Carneiro and A. Berry. Unsupervised Environmental Sound Source Localization and Acoustic Image Analysis of Geometry-Optimized Spherical Microphone Arrays Using the Generalized Cross-Correlation. In *e-Forum Acusticum 2020*, pages 305–312, Lyon, France, 2020. hal-03231913.

[5] T. Padois, J. St-Jacques, K. Rouard, N. Quaegebeur, and al. Acoustic Imaging with Spherical Microphone Array and Kriging. *JASA Express Lett*, 3(4):042801, 2023.

[6] K. Rouard, J. St-Jacques, F. Sgard, H. Nelisse, and al. Numerical Comparison of Acoustic Imaging Algorithms for a Spherical Microphone Array. In *BeBeC*, Berlin, Germany, 2022.

[7] J. St-Jacques, K. Rouard, F. Sgard, H. Nélisse, and al. Effect of the Error on the Sound Speed and Microphone Position on Acoustic Image Obtainde With a Spherical Microphone Array. volume 50-3, page 132, St. John's, Canada, 2022.

[8] R. H. Hardin and N. J. A. Sloane. McLaren's Improved Snub Cube and Other New Spherical Designs in Three Dimensions. *Discrete & Computational Geometry*, 15(4):429–441, 1996.

[9] H. J. Weber and G. B. Arfken. Chap. 2 - Vector Analysis in Curved Coordinates and Tensors. In *Essential Mathematical Methods for Physicists*. Academic, San Diego, 6th edition, 2003.